Theor Chem Acc (2007) 118:193–201
DOI 10.1007/s00214-007-0274-x

REGULAR ARTICLE

New computational evidence for the catalytic mechanism of carbonic anhydrase

Gian Pietro Miscione · Marco Stenta · Domenico Spinelli · Ernst Anders · Andrea Bottoni

Received: 7 December 2006 / Accepted: 1 February 2007 / Published online: 5 April 2007

Abstract Some aspects of the catalytic mechanism of HCA have been investigated. Either a zinc-bound water or a zinc-bound hydroxide has been considered as a nucleophile attacking CO_2. No reaction path exists in the former case, while a transition state for the nucleophilic attack has been located in the latter (barrier of 7.6 kcal mol^{-1}). This activation energy is determined by the breaking of the hydrogen-bond network that shields the zinc-bound hydroxide when the CO_2 molecule approaches the reaction center. No ambiguity exists about the mechanism for the internal rearrangement of the zinc–bicarbonate complex. The rotation pathway (Lindskog mechanism) proposed by many authors is too energy demanding since it causes the breaking of the hydrogen-bond network around the bicarbonate. The only possible rearrangement mechanism is a proton transfer (Lipscomb) that occurs in two steps (each step corresponding to a double proton transfer) and involves the Thr199 residue as a proton shuttle.

Electronic supplementary material The online version of this article (doi:10.1007/s00214-007-0274-x) contains supplementary material, which is available to authorized users.

Contribution to the Fernando Bernardi Memorial Issue.

G. P. Miscione · A. Bottoni (✉)
Dipartimento di Chimica "G.Ciamician",
Università di Bologna, via Selmi 2, 40126 Bologna, Italy
e-mail: andrea.bottoni@unibo.it

M. Stenta · D. Spinelli
Dipartimento di Chimica Organica "A.Mangini",
Università di Bologna, via S. Giacomo 11, 40126 Bologna, Italy

E. Anders
Institut für Organische Chemie und Makromolekulare Chemie,
Friedrich-Schiller-Universität Jena, Humboldtstrasse 10,
07743 Jena, Germany

Keywords Carbonic anhydrase · Catalytic mechanism · Theoretical study · DFT computations

1 Introduction

Human carbonic anhydrase II (HCA II) is a zinc-based metalloenzyme that catalyzes the reversible hydration of CO_2 to bicarbonate. This enzyme is a single polypeptide chain of 260 aminoacids that catalyzes the reaction with rates up to 10^7 times higher than in the uncatalyzed reaction [1–3]. Thus the reaction has the features of diffusion-controlled processes. As shown by X-ray diffraction [4–7]. the active site is formed by a zinc cation Zn^{2+} in a tetrahedral coordination geometry. The metal is bound to three rigid imidazole groups belonging to three histidine residues (His94, His96 and His119) and a water molecule. One region of the active site (the so-called hydrophilic pocket) contains several water molecules and the His64 residue. This residue is thought to behave as an intra-molecular proton acceptor in the transfer of a proton from the zinc-bound water to an external buffer. Another region (hydrophobic pocket) is characterized by the presence of binding sites involved in the CO_2 transport and the so-called "deep water". In the approaching process to the zinc ion, CO_2 probably displaces this water molecule, which is about 3.2 Å away from the metal.

The almost universally accepted mechanism of HCA II (see Scheme 1) is based on a large number of experimental [1–14] and theoretical [15–32] investigations carried out during the last three decades. It consists of three main steps. The first step involves the proton release from the Zn-bound water to form a Zn–bound hydroxide (see Eq. 1 where *E* indicates the enzyme). In the second step the zinc-bound hydroxide carries out a nucleophilic attack on the CO_2 carbon to form

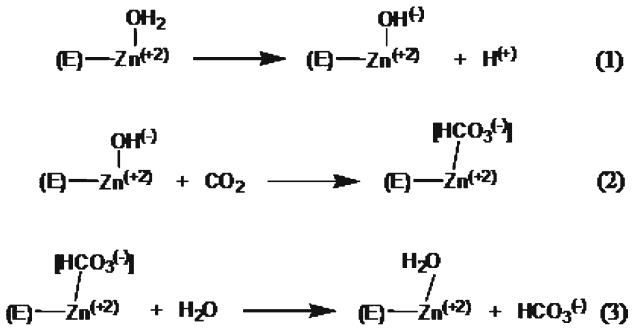

Scheme 1

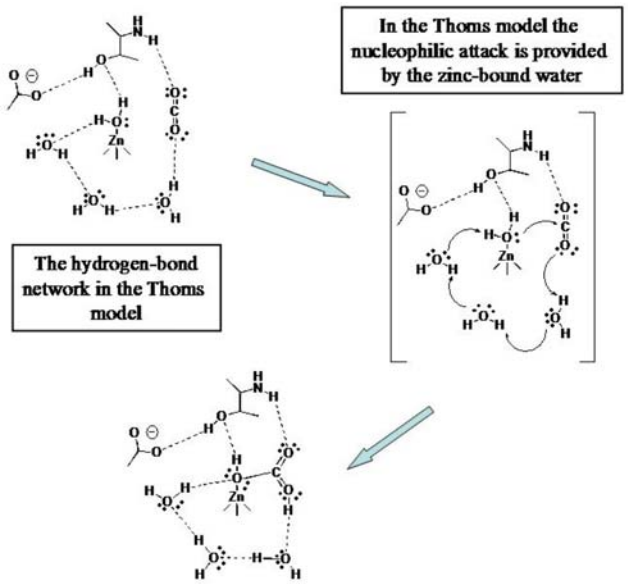

Scheme 2

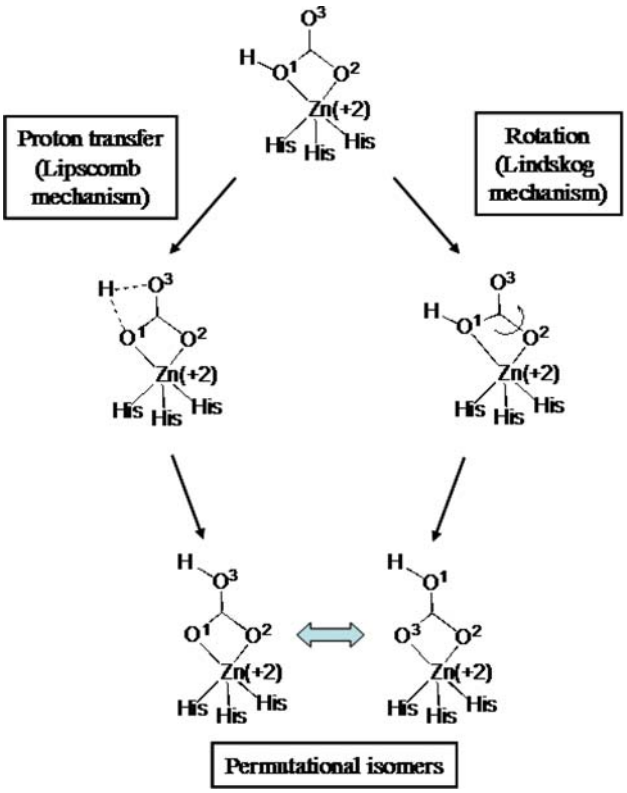

Scheme 3

bicarbonate (Eq. 2). In step 3 an external water molecule replaces the zinc-bound bicarbonate, which is expelled from the metal coordination sphere (Eq. 3) and closes the catalytic cycle.

Thoms proposed a different mechanism, which is schematically represented in Scheme 2 [14]. This author, on the basis of the crystallographic structure of the hydrogen-bond network within the catalytic site, suggested that the zinc-bound water and not the zinc-bound hydroxide, carries the nucleophilic attack on CO_2. Within this mechanism the formation of a low-barrier hydrogen-bond network (LBHB) involving CO_2, would enhance the electrophilic character of carbon dioxide and lower the energy of the transition state for the C–O bond formation. A partial activation of the zinc-bound water (increase of its nucleophilic character) should be determined during the nucleophilic attack by a simultaneous transfer of a proton from this water molecule to another water of the network, as indicated in Scheme 2.

Recently, we carried out a theoretical DFT investigation on the second and third step of the carbonic anhydrase catalytic cycle reported in Scheme 1 [32]. We used a model-system including the Glu106 and Thr199 residues, the "deep water" molecule and a Zn^{2+} cation coordinated to an hydroxide ion and three imidazole rings. We found that the nucleophilic attack of the zinc-bound hydroxide on CO_2 has a negligible barrier, suggesting that this step cannot be the rate-determining step of the process. Also, we examined the mechanism of the internal rearrangement of the zinc–bicarbonate complex (see Scheme 3). We found that the direct intra-molecular proton transfer from the zinc-bound oxygen to another oxygen of the bicarbonate moiety (Lipscomb mechanism) can effectively compete with a rotational mechanism (Lindskog mechanism). These transformations lead to identical permutational isomers. We demonstrated that the proton transfer is a two-step process, which is assisted by a complex network of hydrogen bonds involving Glu106 and Thr199 where the threonine residue acts as a proton shuttle. In the absence of Glu106 the barrier for the proton transfer significantly increases and the rotational (Lindskog) mechanism becomes definitely favored. In that paper we also considered the attack of the water on the zinc–bicarbonate complex (step 3) leading to a penta-coordinate intermediate, but we did not investigate in detail the mechanism of the bicarbonate expulsion.

Our results, indicating a very low barrier for the nucleophilic attack, were in contrast with those obtained by Anders

and co-workers who found a barrier of 5.7 kcal mol^{-1} at the B3LYP level using a smaller model-system (formed by the $[(NH_3)_3Zn(OH)]^+$ complex reacting with CO_2) but a more accurate basis set [30]. On the other hand, the investigation carried out by these authors on the internal bicarbonate rearrangement were in rather good agreement with our model. Their results pointed to the Lindskog-type mechanism (internal rotation) as the most favored path and not to a direct proton shift, characterized by a significantly higher activation energy (about 28 kcal mol^{-1}). Interestingly, this value is rather close to the proton transfer activation barrier that we found in the absence of the Glu106 residue (32 kcal mol^{-1}). We must also outline that the results of our first study [32] on HCA are not in contrast with other investigations, based on solvent isotope effects, which suggest that the rate-determining step of the reaction could be the enzyme activation, i.e., the proton transfer from the zinc-bound water to a proton acceptor (the imidazole ring of the His64 residue) contained in the active site [2,17,31]. The energetics of this proton transfer was accurately examined in a recent paper by Cui and Karplus [31]. They considered different model-systems involving two, three and four water molecules acting as carriers. They demonstrated that the proton transfer process is fully concerted with two water molecules and becomes partially concerted and stepwise with three and four water molecules, respectively. Also, the barrier height increases as the number of water molecules increases (a value of 0.6, 3.6 and about 6 kcal mol^{-1} was calculated for the three different models, respectively). These authors pointed out that a model based on three or four water molecules provides results that are consistent with the experimental kinetic observations.

In the present paper we again investigate the HCA mechanism using a model-system based on Thoms' hypothesis. This has been obtained by adding to our first model [32] the three water molecules involved in the low-barrier hydrogen-bond network evidenced in Thoms' theory. In particular we examine here again (1) the nucleophilic attack using as a nucleophile either a zinc-bound water (as suggested by Thoms) or a zinc-bound hydroxide (the usual active form of the enzyme), (2) the internal bicarbonate arrangement and (3) the final attack of a water molecule that should lead to the expulsion of the bicarbonate fragment from the metal coordination sphere. A detailed analysis of the effect of the hydrogen-bond network on the various reaction steps is given.

2 Computational details and choice of the model

The model-system used here (see Fig. 1) has been assembled using the crystallographic structure available in literature [7]. This model includes: (1) a Zn^{2+} cation bonded to a HO^- group (or, alternatively, a water molecule) and three imidazole rings belonging to the three histidine residues His94, His96 and His119; (2) the Glu106 residue; (3) the Thr199 residue; (4) the four water molecules W318, W338, W359 and W386; (5) a CO_2 molecule. To reduce the size of the model an acetate fragment has been used to emulate the Glu106 residue. Also, we have replaced the threonine with a serine and we have cut the protein backbone along the bonds adjacent to the carbonyl groups.

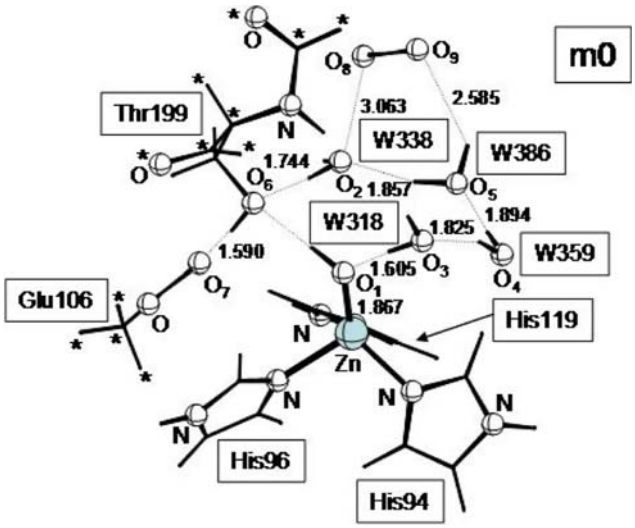

Fig. 1 A schematic representation of the model-system used in this paper (bond lengths in Ångstroms). The reported structure corresponds to that of the preliminary complex m0 (absolute energy = −3694.03761 a.u.). The asterisks indicate the atoms (in addition to those of the imidazole rings) that have been kept frozen during the geometry optimization

As already described in ref. [32], to emulate the partially constraining effect of the protein environment, during the geometry optimization procedure we have not optimized the positions of the atoms not directly involved in the reaction or in hydrogen bond formation. This approach, where a number of appropriately chosen atoms have been anchored to their crystallographic coordinates, preserves the geometry of the active-site cavity. The "frozen" atoms include the three imidazole rings and all the atoms marked by an asterisk in Fig. 1. For the serine (threonine) residue we have not locked the whole CH_2–OH fragment. In this way the OH group should approximately have the same freedom it has in the real enzyme to adjust its position and form effective hydrogen bonds with the neighboring groups.

All the reported DFT computations have been carried out with the Gaussian 03 series of programs [33] using the B3LYP [34] functional and the DZVP basis set [35]. The B3LYP functional has been demonstrated to provide reliable description of systems including transition metals and involving hydrogen bond interactions [32,36–39]. The DZVP basis is a local spin density (LSD)-optimized basis set of double-zeta quality that includes polarization functions and is suitable to describe weak hydrogen interactions such

as those occurring in the system investigated in this paper. The transition vector of the various transition states has been analyzed by means of frequency computations.

The effect of the whole protein environment has been evaluated with the solvent continuous model approach COSMO [40,41] as implemented in the Turbomole package [**Turbomole**, version 5.6, Institut für Physikalische Chemie und Elektrochemie Lehrstuhl für Theoretische Chemie Universität Karlsruhe Kaiserstr. 12 D-76128 Karlsruhe]. The dielectric constant of nitromethane ($\varepsilon = 38.2$) was used. This value should take into account the simultaneous presence of hydrophilic and hydrophobic groups around the active site. A value of about 40 was suggested elsewhere to describe the effect of charge–charge interactions in proteins [42]. Several papers available in literature report the results of the COSMO method in the calculations on enzymatic models and systems involving hydrogen bonds and proton transfers [32,43–46].

3 Results and discussion

In this section we examine in detail the singlet potential energy surface that describes the catalytic cycle of HCA. We consider either the case of a zinc-bound hydroxide or that of a zinc-bound water (Thoms' hypothesis) attacking CO_2. The corresponding energy profile is reported in Fig. 2, while the structures of the various critical points are represented in Fig. 1, 3, 4, 5, 6, 7, 8 and 9.

3.1 The starting complex, the nucleophilic attack and the origin of the barrier

The preliminary complex m0 is depicted in Fig. 1. It provides a schematic representation of the active site with the CO_2 molecule still far away from the reactive center. A chain of hydrogen bonds involves the four water molecules W318, W338, W359 and W386, the zinc-bound hydroxide and the Thr199 residue. All these molecules and groups are arranged in a ring-like structure that shields the zinc-bound hydroxide with respect to the approaching carbon dioxide CO_2. Only a weak hydrogen interaction ($O_9\cdots H$) between CO_2 and W386 can be recognized ($O_9\cdots H(O_5)$ distance = 2.585 Å. (An additional hydrogen bond involves the oxygen atom O_7 of the Glu106 residue and the threonine hydroxide ($O_7\cdots H(O_6)$ distance = 1.590 Å).

A transition state ts1 connects m0 to a new complex m1 (almost degenerate to m0) where CO_2 is still rather far from the zinc-bound hydroxide, but is now oriented in a suitable way for the nucleophilic attack (see Fig. 3). To undertake the transformation m0 → m1 a small barrier of 2.6 kcal mol^{-1} must be overcome. The new position of CO_2 partially breaks the original ring-like structure and W338 is now far-away from W386, the $O_2\cdots H(O_5)$ distance being 4.123 Å. In this new structural arrangement it is possible to recognize a smaller ring-like structure formed by the zinc-bound hydroxide and the three water molecules W318, W359 and W386. Rather strong hydrogen bonds characterize this circular frame around the hydroxide ($O_1\cdots H(O_3)$ = 1.702 Å, $O_3\cdots H(O_4)$ = 2.035Å, $O_5\cdots H(O_4)$ = 1.998Å, $O_1\cdots H(O_5)$ = 1.670Å). CO_2 is partially bound to W386 and Thr199 by two weak hydrogen bonds involving the same oxygen atom O_8 : O_5–H$\cdots O_8$ interaction (H$\cdots O_8$ distance = 2.496 Å) and N − H$\cdots O_8$ interaction (H$\cdots O_8$ distance = 2.778 Å).

In the subsequent step (m1 → ts2 → m2) the zinc-bound hydroxide (nucleophile) attacks CO_2. To move closer to the nucleophile the carbon dioxide molecule breaks the network of hydrogen bonds involving the three water molecules W318, W359 and W386 that "protect" the hydroxide. In the transition state ts2 (see Fig. 4) the $O_5\cdots H(O_4)$ interaction becomes significantly weaker (the $O_5\cdots$ H distance changes from 1.998 in m1 to 2.337 Å in ts2) and the $O_1\cdots H(O_5)$ hydrogen bond is destroyed by the approaching CO_2. The new forming carbon–oxygen bond O_1–C(CO_2) is 2.030 Å, but CO_2 remains strongly anchored to W386 by the $O_8\cdots H(O_5)$ hydrogen interaction ($O_8\cdots$H distance = 2.005 Å). The shorter distance between the substrate and the hydroxide has the effect of bending the linear carbon dioxide molecule, the O_8CO_9 angle being now 155.7°.

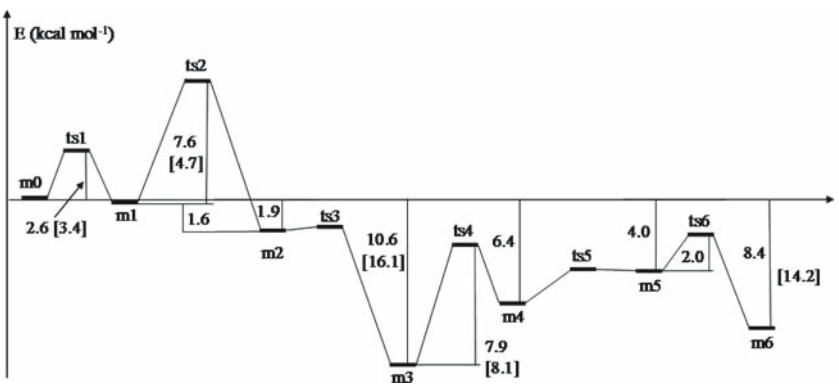

Fig. 2 Energy profile obtained for the HCA catalytic process

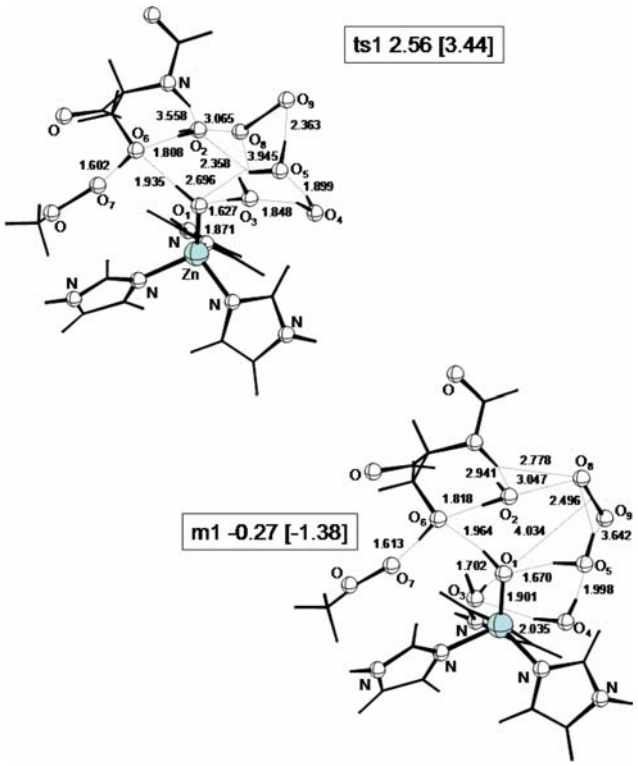

Fig. 3 Schematic representation of the structure of the critical points ts1 and m1 (bond lengths are in Ångstroms). The energy values (kcal mol^1) are relative to m0. Values in brackets have been obtained with the COSMO method

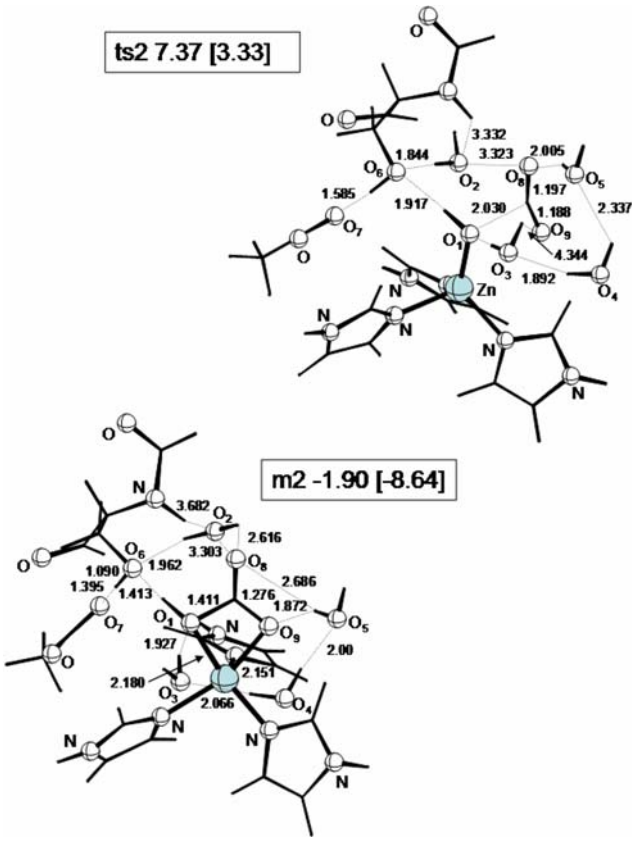

Fig. 4 Schematic representation of the structure of the critical points ts2 and m2 (bond lengths are in Ångstroms). The energy values (kcal mol^{-1}) are relative to m0. Values in brackets have been obtained with the COSMO method

The energy required to break the wall of water molecules around the zinc-bound hydroxide is responsible for the activation barrier computed for ts2 (7.6 kcal mol^{-1}) and explains why an almost negligible barrier (about 1 kcal mol^{-1}) is found when the three water molecules W318, W359 and W386 are missed in the model-system (see ref. [32]). The new energy barrier value found here is in rather good agreement with that found by Anders and co-workers (5.7 kcal mol^{-1}) [29].

The resulting complex m2 is 1.6 kcal mol^{-1} lower in energy than m1. The stabilization of m2 is determined by the restoration of the hydrogen bond network after the nucleophilic attack. These hydrogen bonds form a new round structure now including the just formed bicarbonate fragment bonded to the metal. The HCO_3^- unit chelates the metal giving rise to a penta-coordinated zinc complex which is rather similar to that already described in ref. [32] (the O_1–Zn and O_9–Zn distances are 2.180 and 2.151 Å, respectively). As already observed in our previous study, a strong hydrogen–bond anchors the bicarbonate to the Thr199 hydroxide fragment ($O_6 \cdots H(O_1)$ distance = 1.413 Å).

Furthermore, to verify the Thoms' mechanistic hypothesis we have considered a model-system with a water molecule bonded to the metal in the place of the hydroxide. We have recomputed the structure of the starting complex (m1′), which is depicted in Fig. 5. m1′ is rather similar to m1. The four water molecules form again a ring-like structure involving CO_2, which interacts with one water molecule (W386) and the N–H bond of the Thr199 residue, as suggested in Thoms' model. The major difference between m1 and m1′ is the distance between the CO_2 carbon and the nucleophilic oxygen O_1. In the former case this distance is 4.034 Å, while in m1′ it is much shorter i.e. 2.877 Å . We have investigated for m1′ the reaction channel for the nucleophilic attack. However, in spite of extensive search on the potential surface we could not find any transition state for the formation of the new O–C bond. We observed a rather rapid energy increase when the oxygen of the zinc-bound water was approaching the carbon dioxide. All attempts to locate this critical point drove the search algorithm back to the starting complex with the zinc-bound water far away from CO_2. These results indicate that, even in the presence of the hydrogen-bond network, the electrophilic character of the CO_2 carbon is not enhanced enough to make possible the nucleophilic attack by the metal-bound water. Also, no simultaneous activation of this water

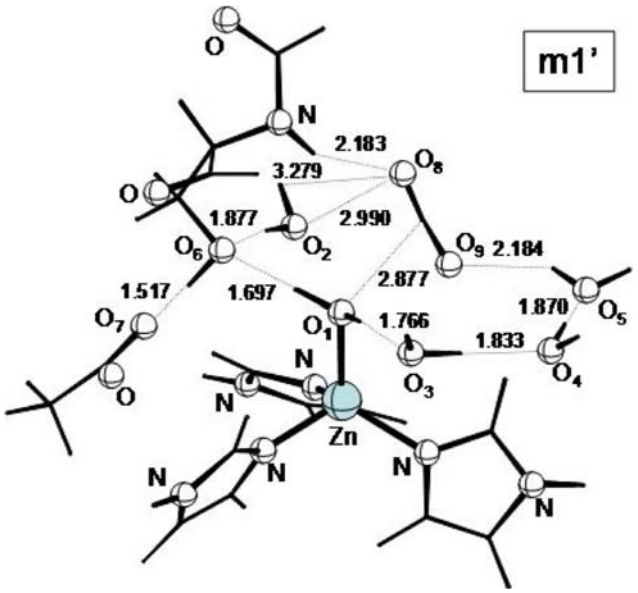

Fig. 5 Schematic representation of the structure of the critical point m1′ (bond lengths are in Ångstroms)

molecule via a partial proton transfer was observed. This evidence makes Thoms' hypothesis quite unlikely.

3.2 The rearrangement of the zinc–bicarbonate complex

We have examined again the rearrangement mechanism of the zinc–bicarbonate complex in the presence of the three additional water molecules considered in the Thoms' model. In spite of extensive search, we did not locate any transition state for the Lindskog mechanism (rotation around the Zn–O_9 bond and simultaneous breaking of the Zn–O_1 bond) and all our attempts to follow this pathway on the potential surface led to a strong energy increase. This finding can be easily understood if we take into account the network of hydrogen bonds that involve the four water molecules and the bicarbonate fragment. Inspection of the structural features of the m2 intermediate clearly shows that the rotation required by the Lindskog mechanism inevitably breaks this network and raises the energy.

The rearrangement can occur rather easily via a double proton transfer mechanism (Lipscomb mechanism). This is very similar to that already discussed in our previous work and requires two subsequent steps where the threonine residue behaves as a proton shuttle. In the first step (m2 → ts3 → m3) a proton is transferred from O_1 (the original hydroxide oxygen) to O_6 of the Thr199 group. Simultaneously the threonine proton is transferred to the Glu106 residue. This transformation leaves the frame of hydrogen bonds roughly unchanged. More precisely, since during the transformation some hydrogen bonds become stronger, ts3 is stabilized and the corresponding barrier becomes negligible (for instance,

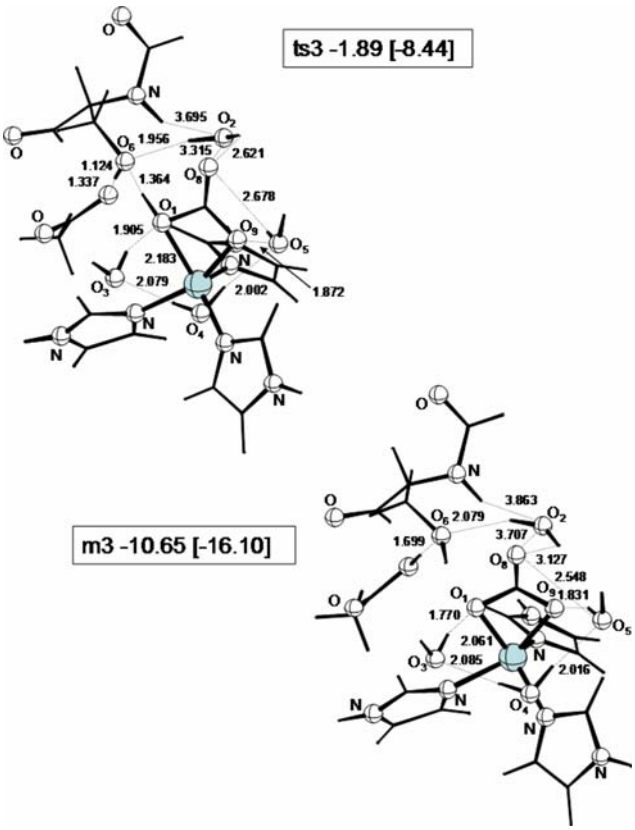

Fig. 6 Schematic representation of the structure of the critical points ts3 and m3 (bond lengths are in Ångstroms). The energy values (kcal mol^{-1}) are relative to m0. Values in brackets have been obtained with the COSMO method

on passing from m2 to ts3 the $O_1 \cdots H(O_3)$ distance changes from 1.927 to 1.905 Å, $O_7 \cdots H(O_6)$ from 1.395 to 1.337 Å and $O_6 \cdots H(O_1)$ from 1.413 to 1.364 Å, see Fig. 6). The second step (m3 → ts4 → m4) corresponds to a double proton transfer in the opposite direction: from Glu106 to Thr199 and from Thr199 to the bicarbonate fragment (ts4 and m4 are depicted in Fig. 7). Since we have a simultaneous breaking of the Zn–O_9 bond and a consequent reorientation of the bicarbonate, the proton is transferred to O_8. Thus, the final effect of the m2 → m4 transformation is an internal proton transfer from O_1 to O_8. The barrier for this second proton transfer is 7.9 kcal mol^{-1}, a value lower than that found in our previous investigation (12.3 kcal mol^{-1}) where we carried out single-point computations, with the same basis set used here, on structures optimized at a lower computational level. The difference can be due to the loss of geometric re-optimization in our previous calculations and to the presence of additional hydrogen bonds in the present model. Thus, these results show that the hypothesis of a Lindskog mechanism is highly unlikely (it is impossible to locate the corresponding pathway on the potential surface since the energy raises very rapidly) and the discussion concerning the competition between

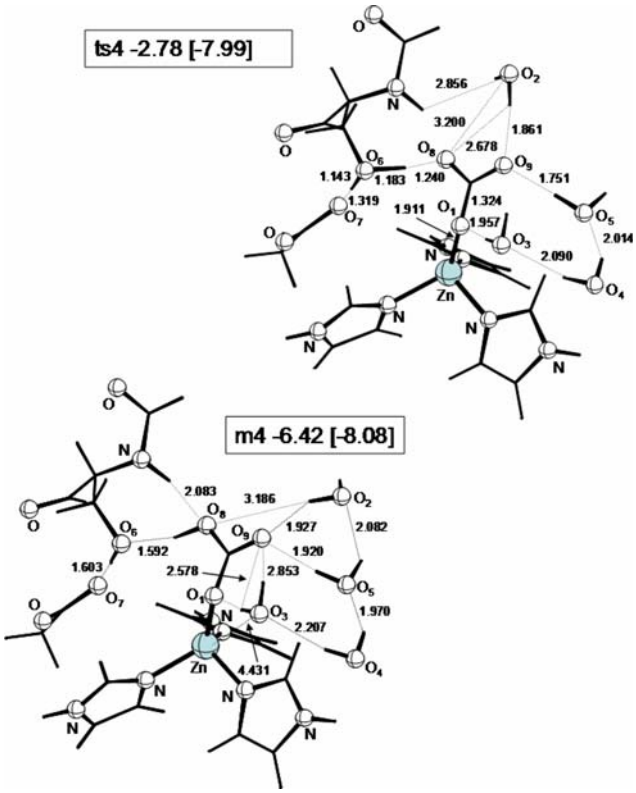

Fig. 7 Schematic representation of the structure of the critical points ts4 and m4 (bond lengths are in Ångstroms). The energy values (kcal mol^{-1}) are relative to m0. Values in brackets have been obtained with the COSMO method

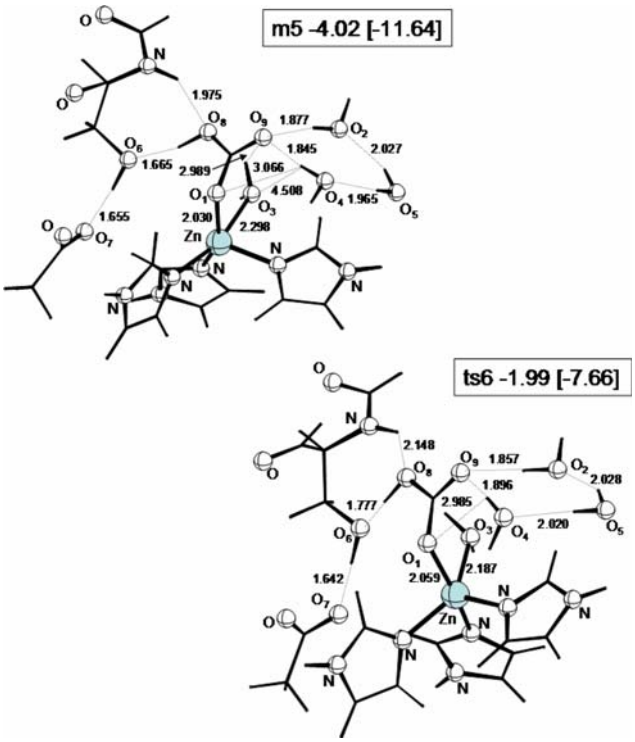

Fig. 8 Schematic representation of the structure of the critical points m5 and ts6 (bond lengths are in Ångstroms). The energy values (kcal mol^{-1}) are relative to m0. Values in brackets have been obtained with the COSMO method

the two possible rearrangement mechanisms (Lindskog vs Lipscomb) is only an academic issue.

3.3 The attack of the water molecule and the formation of a penta-coordinated zinc complex

It is interesting to note that the m4 intermediate is now a four-coordinated complex where one water molecule is correctly oriented to carry out a nucleophilic attack on the metal atom (the distance between the zinc atom and the water oxygen O_3 is 4.431 Å). All the attempts to locate the corresponding transition state (ts5) showed that the transition region is very flat indeed and the search algorithm led in all cases to the penta-coordinated intermediate m5 that results from the water attack (see Fig. 8). Even if it has not been located, ts5 is indicated in the diagram of Fig. 2 and is approximately degenerate to m5. Thus, we again observe that the attack of the water on the metal does not cause the simultaneous expulsion of the bicarbonate fragment but the formation of a new intermediate where both the bicarbonate and the water are firmly bonded to the zinc atom (the two Zn–O_1 and Zn–O_3 bond lengths are 2.030 and 2.298 Å, respectively). The complex m5 is 2.4 kcal mol^{-1} higher in energy than m4. This destabilization (in rather good agreement with the results of ref. [29]) is probably due to the weakening of some hydrogen bonds on passing from m4 to m5 (for instance, $O_3 \cdots H{-}O_4$). Further investigation of the potential energy provides information very similar to that obtained in our first study [32]. The expulsion is a rather complicated process as indicated by the subsequent transformation (m5 → ts6 → m6) characterized by a small barrier of 2.0 kcal mol^{-1}. In the resulting intermediate m6 (see Fig. 9) the bicarbonate–zinc bond is weakened and the water–zinc bond is enforced. More interestingly the bicarbonate hydroxide has changed orientation and points now in the opposite direction. As a consequence the $O_6 \cdots H(O_8)$ hydrogen bond is broken, the bicarbonate fragment is less firmly bound to the Thr199 residue and it should be easier for this fragment to abandon the active site. Thus, the intermediate m6 seems to prepare and organize the real expulsion of the bicarbonate fragment. Since the model-system is still rather small and other residues can play, in principle, an important role in the expulsion process (for instance Thr200 that can anchor the leaving bicarbonate), we did not further investigate the potential surface. Another possibility, which is worth to explore, is the formation of carbonic acid (see ref. [29]) via a proton transfer from O_3 to O_9. This alternative reaction path would have the advantage of leading directly to the enzyme reactivation (formation of

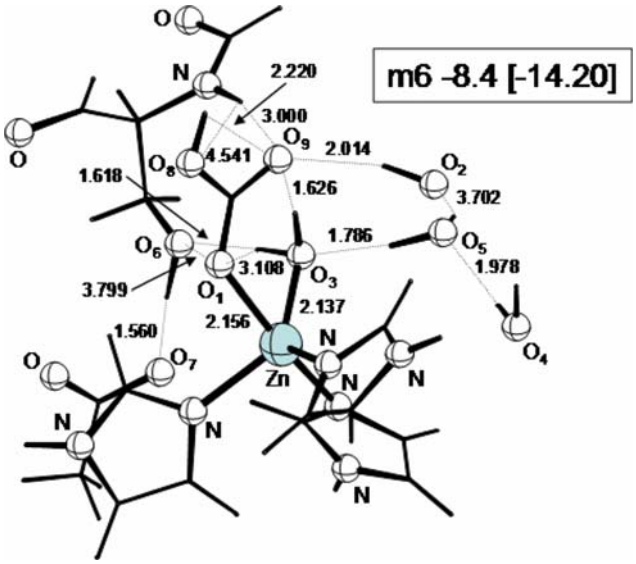

Fig. 9 Schematic representation of the structure of the critical point m6 (bond lengths are in Ångstroms). The energy value (kcal mol^{-1}) is relative to m0. Values in brackets have been obtained with the COSMO method

the nucleophilic zinc-bound hydroxide). Also, H_2CO_3 could leave the field of the Zn^{2+} cation without significant problems.

3.4 The effect of the protein environment

The values of the three largest activation energies (for ts1, ts2 and ts4) and the energy values of the m3 and m6 intermediates obtained in the presence of solvent effects are reported in brackets in Fig. 2. Also, the energy corrected by solvent effects for all the critical points located on the surface are reported in square brackets in Figs. 3–4 and 6–9. The barrier for the nucleophilic attack (m1 → ts2) decreases (from 7.6 to 4.7 kcal mol^{-1}) but this step remains the rate-determining step of the process. In fact the two transition states ts1 and ts2 become almost degenerate (3.4 and 3.3 kcal mol^{-1} above the starting complex m0, respectively), which suggests that in the presence of the protein environment the reorientation of the CO_2 molecule within the active site together with the nucleophilic attack on CO_2, represent the real determining step of the reaction. Interestingly, even if the barrier for ts4 remains almost the same (it changes from 7.9 to 8.1 kcal mol^{-1}), the energy of m3 and m6 become much lower. These two critical points are now 16.1 and 14.2 kcal mol^{-1} lower than m0, respectively. All these results (i.e., the lower barrier for the rate determining step and the larger exothermicity) indicate that the protein environment makes the reaction even faster. This finding is in agreement with the high reaction rate experimentally observed.

4 Conclusions

In this paper some aspects of the catalytic mechanism of HCA have been again investigated using a model-system based on the mechanistic hypothesis proposed by Thoms [14]. This model-system includes three additional water molecules with respect to that examined in ref. [32]. Following this scheme a zinc-bound water and not a zinc-bound hydroxide would carry out a nucleophilic attack on CO_2. The most significant results can be summarized as follows:

(1) Our computational evidence does not support Thoms' hypothesis. We could not locate any transition state for the nucleophilic attack when we have considered as nucleophile a zinc-bound water (as suggested by Thoms) in the place of a zinc-bound hydroxide. Our computations indicate that the presence of the hydrogen bond network is not enough to enhance either the electrophilic character of the CO_2 carbon or the nucleophilic character of the metal-bound water.
(2) A transition state for the nucleophilic attack (with a barrier of 7.6 kcal mol^{-1}) has been located when an activated water (zinc-bound hydroxide) was used as a nucleophile. This activation energy is much larger than that found in our previous study and is determined by the breaking of the hydrogen-bond network when the CO_2 molecule approaches the reaction center.
(3) No ambiguity exists about the mechanism for the bicarbonate rearrangement. The rotation pathway (Lindskog mechanism) is too energy demanding since it causes the breaking of the hydrogen-bond network around the bicarbonate. The only possible rearrangement mechanism is a proton transfer (Lipscomb) that occurs in two steps (each step corresponding to a double proton transfer) and involves Thr199 as a proton shuttle. This mechanism is almost identical to that described in ref. [32] in the absence of the three additional water molecules used here.
(4) The attack of the water on the metal in the zinc–bicarbonate complex (step 2 of Scheme 1) does not cause the simultaneous expulsion of the bicarbonate fragment. On the contrary, we have observed the formation of a penta-coordinated zinc complex where both the bicarbonate and the water are firmly bonded to the metal. Further computations indicate that the expulsion of the bicarbonate is a rather complicated process where other residues that are missed in the present model, could play a key role in stabilizing the leaving group.
(5) The barrier for the nucleophilic attack is comparable to that computed by Karplus [31] for the activation step of the zinc-bound water (a value between 3.6 and 6 kcal mol^{-1}). The accuracy of the computational level used by Karplus (B3LYP/6-31G(d)) is similar to that

employed in the present study. Thus, our results suggest that the nucleophilic attack could be the rate-determining step of the catalytic cycle in agreement with the conclusions reached by Anders and co-workers in ref. [29].

(6) The reaction is exothermic by 8.4 kcal mol^{-1}. This exothermicity value and the low barrier for the nucleophilic attack are consistent with the high reaction speed observed for this catalytic process.

(7) The effect of the protein environment (emulated by solvent continuous model computations) does not change the mechanistic scenario. However, the barrier for the rate-determining step becomes lower and the reaction much more exothermic. This indicates an even faster reaction in agreement with the high reaction rate experimentally observed.

Acknowledgments We would like to thank C.N.R. and M.U.R.S.T. (Progetto Nazionale "Stereoselezione in Sintesi Organica: Metodologie ed Applicazioni") and Bologna University (funds for selected research topics) for the financial support of these researches. E. A. would like to thank the *Deutsche Forschungsgemeinschaft* and the *Fonds der Chemischen Industrie* for financial support.

References

1. Bertini I, Luchinat C (1983) Acc Chem Res 16:272–279
2. Silverman DN, Lindskog S (1988) Acc Chem Res 21:30–36
3. Christianson DW, Fierke CA (1996) Acc Chem Res 29:331–339
4. Woolley P (1975) Nature 258:677–682
5. Liljas A, Kannan KK, Bergsten PC, Waara I, Friborg K, et al. (1972) Nature New Biol 235:131–137
6. Eriksson EA, Jones TA, Liljas A (1986) Zinc enzymes. Birkhaüser, Boston, pp 317
7. Hakansson K, Carlsson M, Svensson LA, Liljas A (1992) J Mol Biol 227:1192–1204
8. Kimura E (2001) Acc Chem Res 34:171–179
9. Huang C, Lesburg CA, Kiefer LL, Fierke CA, Christianson DW (1996) Biochemistry 35:3439–3446
10. Lesburg CA, Huang CC, Christianson DW, Fierke CA (1997) Biochemistry 36:15780–15791
11. Zhang X, Hubbard CD, van Eldik R (1996) J Phys Chem 100: 9161–9171
12. Nair SK, Calderone TL, Christianson DW, Fierke CA (1991) J Biol Chem 266:17320–17325
13. Tu C, Tripp BC, Ferry JG, Silverman DN (2001) J Am Chem Soc 123:5861–5866
14. Thoms S (2002) J Theor Biol 215:399–404
15. Liang JY, Lipscomb WN (1986) J Am Chem Soc 108:5051–5058
16. Liang JY, Lipscomb WN (1987) Biochemistry 26:5293–5301
17. Merz KM, Hoffmann R, Dewar MJS (1989) J Am Chem Soc 111:5636–5649
18. Liang J-Y, Lipscomb WN (1989) Int J Quantum Chem 36:299–312
19. Jacob O, Cardenas R, Tapia O (1990) J Am Chem Soc 112: 8692–8705
20. Krauss M, Garmer DR (1991) J Am Chem Soc 113:6426–6435
21. Zheng YJ, Merz KM (1992) J Am Chem Soc 114:10498–10507
22. Sola M, Lledos A, Duran M, Bertran J (1992) J Am Chem Soc 114:869–877
23. Sakurai M, Furuki T, Inoue Y (1995) J Phys Chem 99:17789–17794
24. Murcko MA (1997) Theor Chem Acc 96:56–60
25. Merz KM, Banci L (1997) J Am Chem Soc 119:863–871
26. Lu D, Voth GA (1998) J Am Chem Soc 120:4006–4014
27. Toba S, Colombo G, Merz KM (1999) J Am Chem Soc 121: 2290–2302
28. Denisov VP, Jonsson BH, Halle B (1999) J Am Chem Soc 121:2327–2328
29. Mauksch M, Bräuer M, Weston J, Anders E (2001) Chem Bio Chem 2:190–198
30. Brauer M, Perez-Lustres JL, Weston J, Anders E (2002) Inorg Chem 41:1454–1463
31. Cui Q, Karplus M (2003) J Phys Chem B 107:1071–1078
32. Bottoni A, Lanza CZ, Miscione GP, Spinelli D (2004) J Am Chem Soc 126:1542–1550
33. Frisch MJ. 2004. Gaussian 03, Revision C.02; Gaussian, Inc., Wallingford CT, 2004. Full authors citation is provided in Supporting Information
34. Becke AD (1993) J Chem Phys 98:1372–1377
35. Godbout N, Salahub DR, Andzelm J, Wimmer E (1992) Can J Chem 70:560–571
36. Ziegler T (1991) Chem Rev 91:651–667
37. Geerlings P, De Proft F, Langenaeker W (2003) Chem Rev 103:1793–1873
38. Bernardi F, Bottoni A, Miscione GP (2001) Organometallics 20:2751–2758
39. Bottoni A, Higueruelo AP, Miscione GP (2002) J Am Chem Soc 124:5506–5513
40. Klamnt A (1995) J Phys Chem 99:2224–2235
41. Klamnt A (1996) J Phys Chem 100:3349–3353
42. Warshel A, Naray-Szabo G, Sussman F, Hwang J-K (1989) Biochemistry 28:3629–3637
43. Lau EY, Newby ZE, Bruice TC (2001) J Am Chem Soc 123:3350–3357
44. Bach RD, Thorpe C, Dmitrenko O (2002) J Phys Chem B 106:4325–4335
45. Keeffe JR, Gronert S, Colvin ME, Tran NL (2003) J Am Chem Soc 125:11730–11745
46. Chocholousova J, Vacek J, Hobza P (2003) J Phys Chem A 107:3086–3092